Journal of Power Sources, 22 (1988) 133 - 148

I — KINETICS OF REDUCTION OF MANGANESE DIOXIDE BY ASCORBIC ACID AND HYDRAZINE SOLUTIONS

M. W. ROPHAEL*, N. S. PETRO and L. B. KHALIL

The National Research Centre, Dokki, Cairo (Egypt)

(Received February 11, 1987; in revised form July 10, 1987)

Summary

The reduction rates of 7 commercial (4 γ-MnO_2 and 3 ϵ-MnO_2) and 5 prepared MnO_2 samples by ascorbic acid solution at 25 °C have been determined and the second-order kinetics with respect to ascorbic acid observed. The activation enthalpy and entropy for the reduction of two of the samples (ICS5 and R2) by ascorbic acid were: 31.5 and 20.5 kJ mol^{-1} and −154 and −210 J mol^{-1} K^{-1}, respectively. The nitrogen liberation rates in the N_2H_4/MnO_2 reaction, generally indicative of the battery activity, were studied using the same samples. The results suggested that the kinetics were dependent on the surface area of the powders and the diffusion of protons into the lattice as influenced by the crystallographic structure. The faster rate of reduction at the lower pH values indicated acid catalysis. The reduction of the different size fractions of one of the samples (ICS4) showed that the real, rather than the BET, surface area played a significant role. Generally, doping the prepared samples led to an increase in the rate of reduction by ascorbic acid and by hydrazine. An increase in the rate of reduction by both ascorbic acid and hydrazine with an increase in the BET surface area was also observed.

1. Introduction

Manganese dioxide is a unique oxide because both protons and electrons can move freely within the oxide structure to form a one-phase, solid, redox system. The dioxide is known to be reduced chemically by the electron–proton mechanism. Ascorbic acid solutions acidified with concentrated hydrochloric acid were found to dissolve MnO_2 more readily than oxalic acid solutions. Different reagents have been reported for titrating ascorbic acid solutions [1] but reproducible tittration results were obtained

*Author to whom correspondence should be addressed.

*Present address: Mid-Kent College of Higher and Further Education, Horsted, Chatham, Kent ME5 9UQ, U.K.

0378-7753/88/$3.50

using Mn^{III} solution [2]. The kinetics and mechanism of reduction of $KMnO_4$ by L-ascorbic acid in H_2SO_4 medium have recently been reported [3].

The reduction of γ-MnO_2 by hydrazine has been found to involve a phase reaction with lattice expansion [4], due to the formation of Mn^{III} ions in the lattice [5, 6]. The mechanism of chemical reduction by N_2H_4 was thought to be similar to the electrochemical reduction [7]. Measurements of the reduction rates of manganese dioxides by hydrazine have been suggested as a means of assessing their battery activity [8]. The effect on the rate of reduction with hydrazine by doping MnO_2 with cations of valency higher and lower than 4 has been reported [9, 10]. Two different mechanisms were suggested for the reduction of γ-MnO_2 by $N_2H_4 \cdot H_2O$ solution, depending on the degree of reduction [11].

2. Experimental

Seven samples of manganese dioxide — three International Common Samples (ICS), one commercially electrodeposited (γ-MnO_2) and three fibrous electrodeposited (ϵ-MnO_2) — were investigated. Four manganese dioxide samples were doped with Specpure Mo^{VI} and Ga^{III} cations and together with an undoped sample were prepared as described previously [12]. The fibrous doped and undoped samples were crushed and then ground to pass through an ASTM 75 μm sieve. The other samples used in this study were "as supplied" except where otherwise stated. The solids were characterised by chemical analysis using a modified Gattow's method [13, 14], by powder X-ray diffraction, and by their specific surface areas determined by the nitrogen adsorption method (Table 1).

2.1. Reduction of manganese dioxides using ascorbic acid

The kinetics of MnO_2 reduction by ascorbic acid solutions were followed using a double-walled beaker, as shown in Fig. 1 [15]. Two grams of powdered MnO_2 were added to 150 ml of a 0.1 M ascorbic acid solution, freshly prepared in boiled distilled water. This was held at 25 ± 0.5 °C for 20 min, while being stirred magnetically and with a constant flow of nitrogen through the inlet (B) and the outlet (C). At given time intervals, some of the solution was sucked through a G4 sintered glass disc (D) into the tube (E). After pipetting 5.0 ml of the filtrate, the remainder was returned to the bulk solution by applying pressure through (F). The 5.0 ml aliquot was acidified with 3 M H_2SO_4 and titrated with a standardised, freshly prepared, Mn^{III} solution using ferroin as the indicator [16]. Stable Mn^{III} solutions, prepared in excess Mn^{II} and excess acidity, were kept in a dark, stoppered bottle at about 5 °C and standardised shortly before the end of a kinetic run by titrating with 0.01 M $FeSO_4$ solution (freshly prepared from a standardised 0.1 M solution again using the ferroin indicator). For each kinetic run, 5.0 ml aliquots from the original 0.1 M ascorbic acid solution

TABLE 1

Characteristics of the used MnO_2 samples

No.	Sample	Type	1 + x	Composition				Surface area ($m^2\ g^{-1}$) BET method
				Total Mn (%)	MnO_{1+x} (%)	H_2O (110 °C) (%)	H_2O (400 °C) (%)	
1	ICS4	γ-electrolytic	1.86_2	59.6	91.1	2.7	5.0	53
2	ICS5	γ-chemical	1.88_2	59.9	92.7	1.8	2.6	71
3	ICS12	γ-chemical	1.93_4	61.5	96.1	1.5	4.3	90
4	R2	γ-electrolytic	1.94_8	59.3	92.9	1.7	4.7	57
5	FEMD-S[a]	ε-electrolytic	1.92_9	58.2	90.9	3.6	6.6	52
6	FEMD-P[b]	ε-electrolytic	1.90_8	61.5	95.7	2.9	5.8	48.5
7	FEMD-N[c]	ε-electrolytic	1.93_4	60.9	95.2	2.8	5.9	45
8	Mo^{VI}-doped (0.03 at.%)	β-MnO_2 with ε-MnO_2 and α-Mn_2O_3	1.89	62.1	96.1	0.2	0.47	3.2[d]
9	Mo^{VI}-doped (0.06 at.%)		1.86_5	61.7	95.2	0.04	0.45	2.9[d]
10	Mo^{VI}-doped (0.09 at.%)		1.80_8	61.4	93.7	0.02	0.44	2.8[d]
11	Ga^{III}-doped (0.1 at.%)		1.82_4	61.5	94.2	0.02	0.42	3.2[d]
12	undoped		1.78_6	59.9	91.1	0.04	0.38	1.6[d]

[a], [b], [c] Precipitated by anodic oxidation from acidic solutions of manganese(II) sulphate (S), perchlorate (P) or nitrate (N).
[d] Calculated from the monolayer capacity at $P/P_0 = 0.1$.

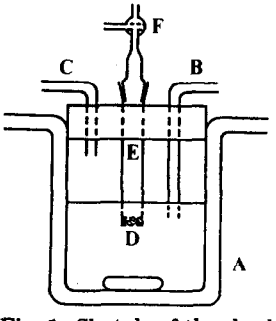

Fig. 1. Sketch of the double-walled beaker used for ascorbic acid reaction.

were similarly titrated. The Mn^{III} titres were used to calculate the molarity of the unreacted ascorbic acid and, hence, the concentration of the ascorbic acid which reacted with MnO_2. Kinetic runs were repeated at three other temperatures to determine the activation parameters for the reduction of the R2 and ICS5 samples.

2.2. Reduction of manganese dioxides using hydrazine

The kinetics of the reduction of manganese dioxide by hydrazine solution were followed by recording the volume of nitrogen evolved against time, using the assembly in Fig. 2. A sample of MnO_2 weighing 2.0 g was suspended in 20 ml of water at 25.0 °C in a 50 ml conical flask (A) and magnetically stirred. A hydrazine solution (20 ml), obtained by a fifty-fold dilution of a Merck $N_2H_4 \cdot H_2O$ solution, was pipetted into flask (B). The hydrazine solution was then added to the MnO_2 suspension by rotating the ground joint at (C) by 180° and inverting flask (B). The gas evolved was collected through (D) in a 100 ml Exelo syringe (E). A slide wire potentiometer (F) monitored the movement of the syringe plunger and generated a signal to drive the chart recorder (H). A record started as the hydrazine solution was added to the MnO_2 suspension and continued until the rate of change became negligible. When the nitrogen evolution was no longer detectable by the wire potentiometer, a micro-burette filled with water was attached to the side tube (D) in Fig. 2 via a polyethylene tube. Monitoring then continued until even this could not detect any change in the volume of nitrogen.

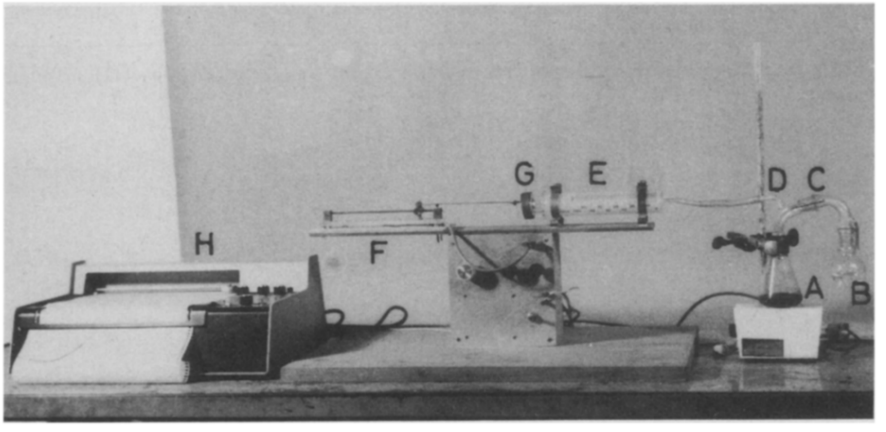

Fig. 2. Photograph of the assembly used in collecting and recording the gas liberated in the kinetic run using hydrazine.

3. Results and discussion

3.1. Reduction using ascorbic acid

Aliquots of the ascorbic acid solution, filtered from the reaction mixture with MnO_2, were titrated against a freshly prepared, standardised Mn^{III} solution. The reaction involved may be represented by:

$$2Mn^{3+} + C_6H_8O_6 = C_6H_6O_6 + 2H^+ + 2Mn^{2+} \quad (1)$$

The concentrations of ascorbic acid solution were calculated after given acid/solid reaction times, and a plot of $x/a(a-x)$ with time was found to be linear. a is the initial concentration of ascorbic acid and $a-x$ its concentration after time t. The linearity of the plots shows that the reaction was second-order with respect to ascorbic acid concentration. Figures 3 - 5 depict the variation of $x/a(a-x)$ with t at 25 °C for γ-MnO_2, ϵ-MnO_2, and the doped and undoped MnO_2 samples which we prepared. The second-order rate constants for the different MnO_2 samples, calculated from the slopes of the lines in Figs. 3 - 5, are presented in Table 2. The increase in the reaction rate with increasing BET surface area is clear from Figs. 3 and 4 and Table 1. The rate does not, however, increase linearly with the surface area. This is not surprising in view of the differences in crystalline form, method of preparation, and impurity levels in the samples studied. In the case of the prepared doped and undoped dioxides (Fig. 5), no clear relation between the reduction rate and the surface area was observed, possibly due to the difference in the level of doping. The reduction rates of all of the doped samples, however, were higher than that of the undoped sample, which had a lower surface area.

It is notable that the two chemically prepared samples, ICS12 and ICS5, were reduced at a higher rate than the electrolytic samples, ICS4 and R2, as shown from Fig. 3. This observation is in line with the reported result that chemical MnO_2 (CMD) shows a higher cation-exchange rate than electrolytic MnO_2 (EMD) [17].

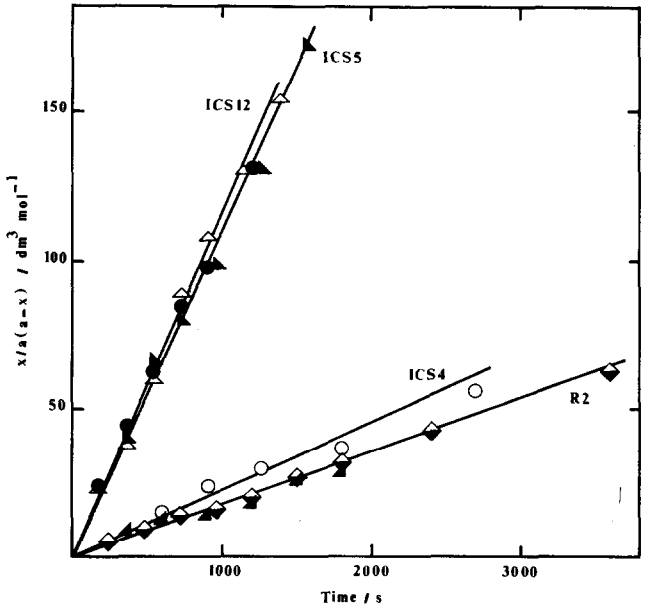

Fig. 3. Variation of $x/a(a-x)$ with time t, for the reaction between ascorbic acid solution at 298.2 K and the different γ-MnO_2 samples; a = initial ascorbic acid concentration; $a-x$ = ascorbic acid concentration at time t.

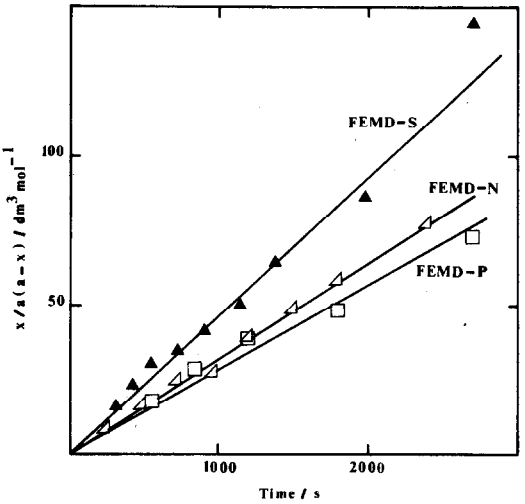

Fig. 4. Variation of $x/a(a-x)$ with time t, for the reaction between ascorbic acid solution at 298.2 K and the different fibrous samples; a = initial ascorbic acid concentration; $a-x$ = ascorbic acid concentration at time t.

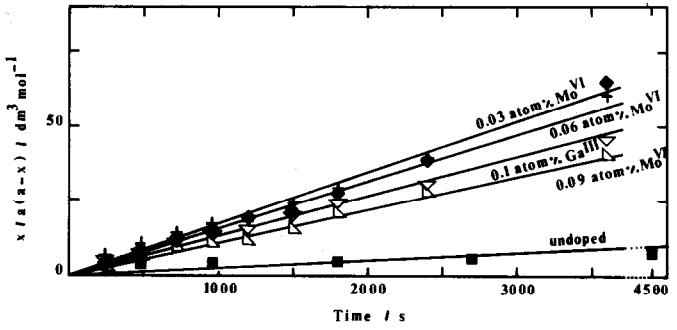

Fig. 5. Variation of $x/a(a-x)$ with time t, for the reaction between ascorbic acid solution at 298.2 K and doped manganese dioxides with different levels of doping; a = initial ascorbic acid concentration; $a-x$ = ascorbic acid concentration at time t.

Increasing the amount of sample from 2.0 g to 4.0 g had no influence on the rate constant per unit surface area (k_r = 1.51 and 1.49×10^{-4} dm^3 mol^{-1} s^{-1} m^{-2}, respectively). This result implies that the role of the reaction at the surface is the dominant factor.

The results of kinetic runs at temperatures of 281.2, 286.2, 291.2 and 298.2 K for ICS5 and R2 are shown in Figs. 6 and 7, respectively. The second-order rate constant, k_r, at the different temperatures, was calculated in each case from the slopes of the lines in Figs. 6 and 7. Its increase with temperature was greater in the case of ICS5 than R2. The activation enthalpy, $\Delta H^{\ddagger}$, and activation entropy, $\Delta S^{\ddagger}$, for the reduction

TABLE 2

Rates of reduction of the different MnO_2 samples by ascorbic acid and hydrazine solutions

Sample No. (as in Table 1)	Ascorbic acid at 25 °C 10^2 × rate constant $dm^3\ mol^{-1}\ s^{-1}\ g^{-1}$ (absolute values)	Hydrazine at 20 °C initial rate $ml\ s^{-1}\ g^{-1}$ (approx. values)
1	1.14	2.9
2	5.20	2.5
3	0.58	5.0
4	0.86	1.6
5	2.30	12.9
6	1.40	3.4
7	1.59	4.7
		10^3 × initial rate $ml\ s^{-1}\ g^{-1}$ (absolute values)
8	0.85	4.17
9	0.78	2.09
10	0.54	0.73
11	0.65	1.79
12	0.12	0.37

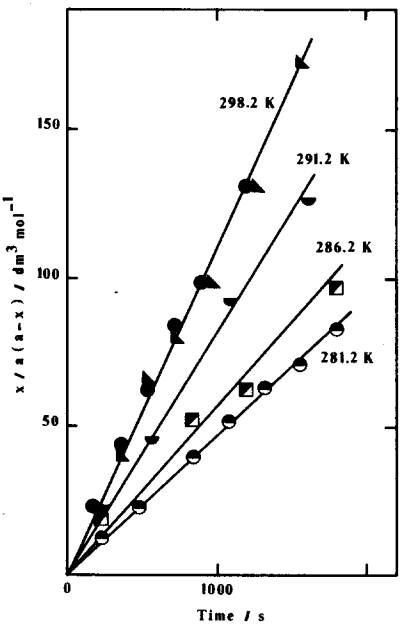

Fig. 6. Variation of $x/a(a-x)$ with time t, for the reaction between ascorbic acid solution and ICS5 at different temperatures; a = initial ascorbic acid concentration; $a-x$ = ascorbic acid concentration at time t.

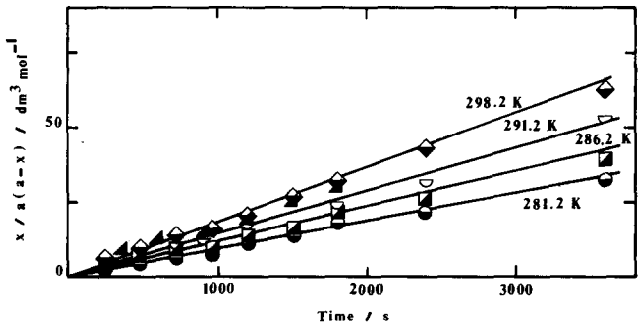

Fig. 7. Variation of $x/a(a-x)$ with time t, for the reaction between ascorbic acid solution and R2 at different temperatures; a = initial ascorbic acid concentration; $a-x$ = ascorbic acid concentration at time t.

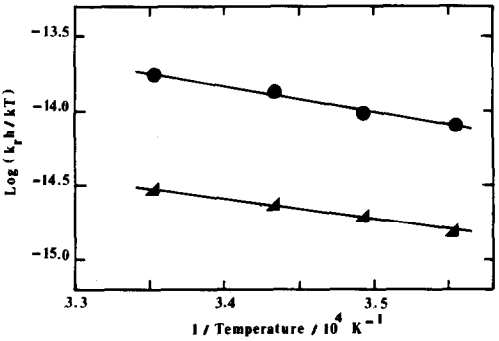

Fig. 8. Variation of $\log(k_T h/kT)$ with $1/T$ for the reaction between ascorbic acid solution and ICS5 (●) or R2 (▲).

of ICS5 and R2, were calculated from the slopes and intercepts of the Eyring plots (Fig. 8). These were 31.5 and 20.5 kJ mol^{-1} and −154 and −210 J mol^{-1} K^{-}, respectively, and are of the same order of magnitude as those for the reaction between ascorbic acid and potassium permanganate [3], namely 31.1 kJ mol^{-1} and −165 J mol^{-1} K^{-1}. The low value for $\Delta H^{\ddagger}$ is not unexpected in ascorbinometric reaction processes [18, 19]. The large negative value for $\Delta S^{\ddagger}$ reported [3] has been ascribed to a more compact structure of the transition state. It was not possible to derive a clear-cut mechanism for the reaction from the results obtained. As the thermodynamic parameters are similar, whether the oxidant is solid MnO_2, or $KMnO_4$ in solution, a rate-limiting process associated only with ascorbic acid is, perhaps, implied.

3.2. Reduction by hydrazine

The experimental results involving the reduction of different γ- and ϵ-MnO_2 samples by hydrazine hydrate solution at 20 °C are shown in Figs. 9 and 10, where the volume of nitrogen liberated is recorded as a

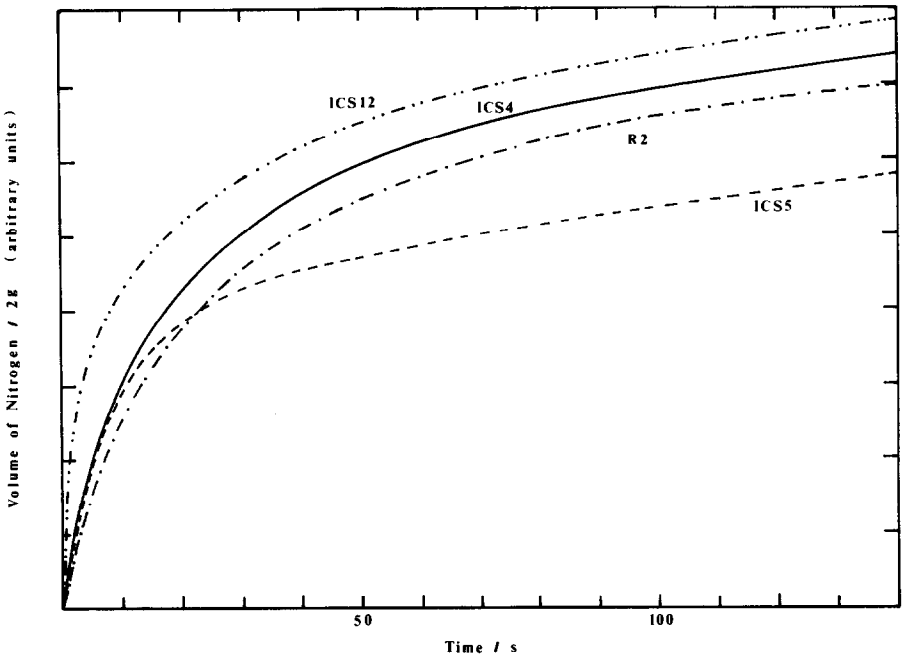

Fig. 9. Kinetic curves for the variation with time of the volume of nitrogen liberated by the reaction of hydrazine solution at 20 °C and the different γ-MnO_2 samples; $[N_2H_4 \cdot H_2O] = 3.66_5 \times 10^{-1}$ mol dm^{-3}.

function of time. The apparatus was not calibrated in absolute values as it was unnecessary for the purpose of comparison, but the error in the relative values of the volume did not exceed ±3.7%. Reproducible results were obtained for a series of runs performed over a short period. Consideration of Figs. 3 and 9 shows that the rate of reduction of the different γ-MnO_2 samples by hydrazine solution followed the same pattern as the rate of reduction with ascorbic acid solution, except for ICS5. This similarity is interesting since MnO_2 was reduced to Mn^{II} by ascorbic acid, where $MnC_2O_4 \cdot 2H_2O$ was isolated from the reaction mixture [20]. The reduction of MnO_2 by hydrazine, however, eventually leads to the formation of δ-MnOOH. Two different mechanisms were suggested in which the filling of the MnO_2 lattice by protons and electrons proceeds differently [11]. The rate of heterogeneous reactions is expected to depend on the adsorption of the solute on the surface [7], the redox reaction at the interface, and the desorption of the products [21]. Additionally, the relative amounts of structural water have a marked effect on the reduction rate of the fibrous, doped, and undoped samples by hydrazine. The effect is less evident in the case of the γ-MnO_2 samples (Tables 1 and 2).

A comparison of Figs. 9 and 10 shows that the ϵ-MnO_2 samples (FEMD-S and FEMD-N) have higher reduction rates than the γ-MnO_2 samples. The reported higher electrochemical reactivity of ϵ-MnO_2 compared with γ-MnO_2

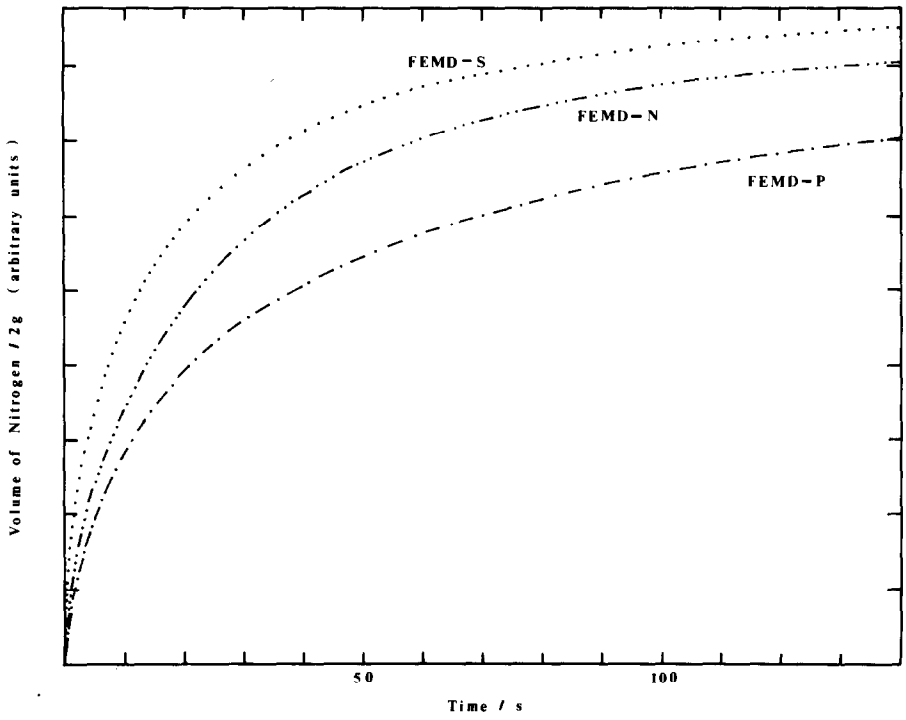

Fig. 10. Kinetic curves for the variation with time of the volume of nitrogen liberated by the reaction of hydrazine solution at 20 °C and the different fibrous samples; $[N_2H_4 \cdot H_2O] = 3.66_5 \times 10^{-1}$ mol dm^{-3}.

[22] suggests that the crystallographic structure plays an important role in determining the electrochemical reduction rate. It is likely that the crystallographic structure also determines the rate of chemical reduction by hydrazine. It has been shown that a parameter, $S\sqrt{D}$ (where S is the surface area and D is the proton diffusion coefficient in the crystal), characterises the depolarising activity of several MnO_2 samples of different crystallographic structure [6]. Consideration of Figs. 4 and 10 shows that the rate of reduction of the fibrous samples by hydrazine solution was highest for FEMD-S and lowest for FEMD-P, as in the case of reduction by ascorbic acid solution.

Since the volumes of nitrogen evolved during the reduction of the prepared doped and undoped samples were quite small, they were measured using a micro-burette, filled with water to ±5%. Figure 11 illustrates kinetic curves for the reduction of the prepared doped and undoped MnO_2 samples by hydrazine solution. Doping manganese dioxide led to an increase in the nitrogen evolution rate by the hydrazine reaction compared with the undoped sample. A similar result was also reported [9] in the case of MnO_2 doped with cations of valency higher than 4. The higher reactivity of the Mo^{VI}-doped sample in the hydrazine reaction is in agreement with the

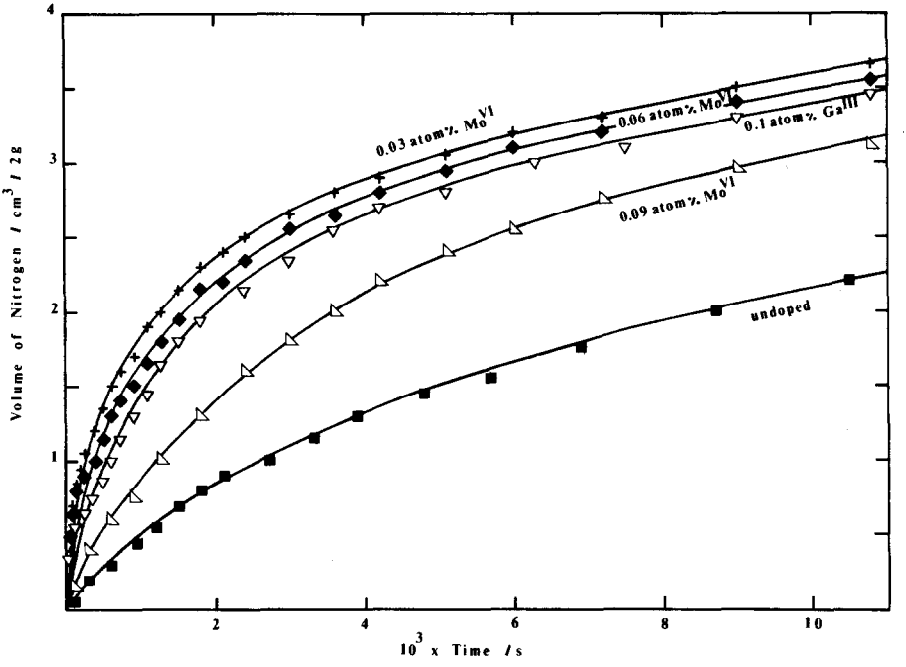

Fig. 11. Kinetic curves for the variation with time of the volume of nitrogen liberated by the reaction of hydrazine solution at 20 °C and doped manganese dioxides with different levels of doping; $[N_2H_4 \cdot H_2O] = 3.66_5 \times 10^{-1}$ mol dm^{-3}.

literature [23, 24], where this effect was ascribed to the more diffuse structure of the Mo^{VI}-doped MnO_2. In general, it is expected that the reactivity of the dioxide samples in hydrazine may depend on the mobility of protons in the samples. The reduction rate of the Mo^{VI}-doped samples by hydrazine, however, decreased as the level of doping increased (Fig. 11). It has been reported that the amount of available oxygen decreased towards a limit with increasing amounts of Mo^{VI} in the MnO_2 [23], suggesting that the molybdenum may be sequestering some of the available oxygen. It is possible that Mo^{VI} creates oxygen vacancies or promotes manganese ions into interstitial positions. It is significant that the rate of reduction of the different Mo^{VI}-doped and undoped MnO_2 samples by hydrazine solution increased as their BET surface areas increased, although the kinetic curves are close to each other.

The initial reduction rates of the different MnO_2 samples by hydrazine (Figs. 9 - 11) are included in Table 2. The lower reduction rates of the doped and undoped MnO_2 samples, compared with the γ-samples, can be correlated with the diffusion of protons in the two types of structure. The small tunnels between the single chains of linked $[MnO_6]$ octahedra of pyrolusite lead to a considerably slower rate of proton diffusion compared with γ-MnO_2 whose structure consists of domains of single and double chains [25].

The initial reduction rates of ICS4 by hydrazine solutions of different concentrations (1.83, 3.66_5 and $5.43_5 \times 10^{-1}$ mol dm^{-3}*), calculated from the initial slopes of the kinetic curves, were used to calculate the actual order of the reaction. A log/log plot of hydrazine concentration *versus* initial reduction rate was found to be a straight line (Fig. 12). The order of the reaction, calculated from its slope, was almost unity, *i.e.*, the reaction was first-order with respect to hydrazine at the initial stages. An overall second-order for the reaction between γ-MnO_2 and hydrazine solution has been found [26], and a bimolecular reaction was suggested but the limited results reported cannot be considered to be conclusive.

From a postulated mechanism for the electrolytic oxidation of hydrazine [27] and assuming that the reduction rate of γ-MnO_2 by N_2H_4 depends on the adsorption of the solute on the surface [7], a scheme of reactions for the oxidation of hydrazine by MnO_2 may be represented by:

$$N_2H_{4(ad)} + OH^- \xrightarrow{\text{slow}} N_2H_{3(ad)} + H_2O + e^- \quad (2)$$

$$N_2H_{3(ad)} \longrightarrow N_2 + 3H_{(ad)} \quad (3)$$

$$3H_{(ad)} + 3OH^- \longrightarrow 3H_2O + 3e^- \quad (4)$$

with the overall reaction being:

$$N_2H_{4(ad)} + 4OH^- \longrightarrow N_2 + 4H_2O + 4e^- \quad (5)$$

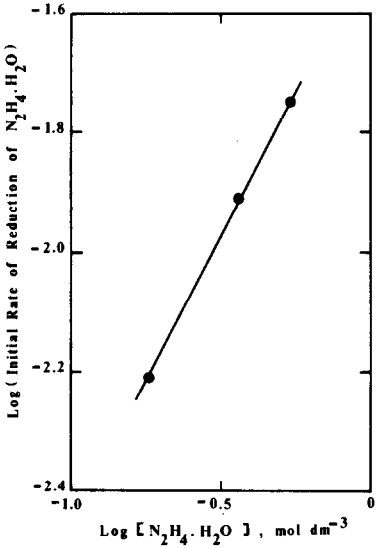

Fig. 12. Log/log plot of the initial rate of reduction of ICS4 by hydrazine solution at 20 °C *vs.* molar concentrations of hydrazine.

*The hydrazine concentration was determined by titration against a standard solution of KIO_3.

It has been suggested that reaction (5) occurs during the reduction of MnO_2 by hydrazine hydrate solution [8]. The molar ratio of $MnO_2 \cdot N_2H_4$ used in ref. 26 was 4:1, in agreement with reaction (5). Thus the electrochemical or chemical reduction of MnO_2 may be represented by:

$$MnO_2 + H^+ + e^- \longrightarrow MnOOH \qquad (6)$$

i.e.,

$$Mn^{4+} + e^- \longrightarrow Mn^{3+}$$

The effect which the pH of the medium has on the rate of reduction of ICS4 by hydrazine was checked at pH values in the range 4.5 - 12.2. In control experiments, each 2 g of ICS4 were suspended in 20 ml of H_2O (pH 8.94). The pH of each suspension was either raised to 12.15 by adding concentrated ammonia solution, or lowered to 6.49 or 4.56 by adding 1 M HCl solution. Twenty millilitres of a $3.66_5 \times 10^{-1}$ mol dm^{-3} $N_2H_4 \cdot H_2O$ solution were added to each suspension at the adjusted pH value and the nitrogen evolved in each case was recorded as a function of time. Figure 13 shows the effect which varying the pH of the medium has on the reduction rate of ICS4 by the same concentration of hydrazine at 20 °C.

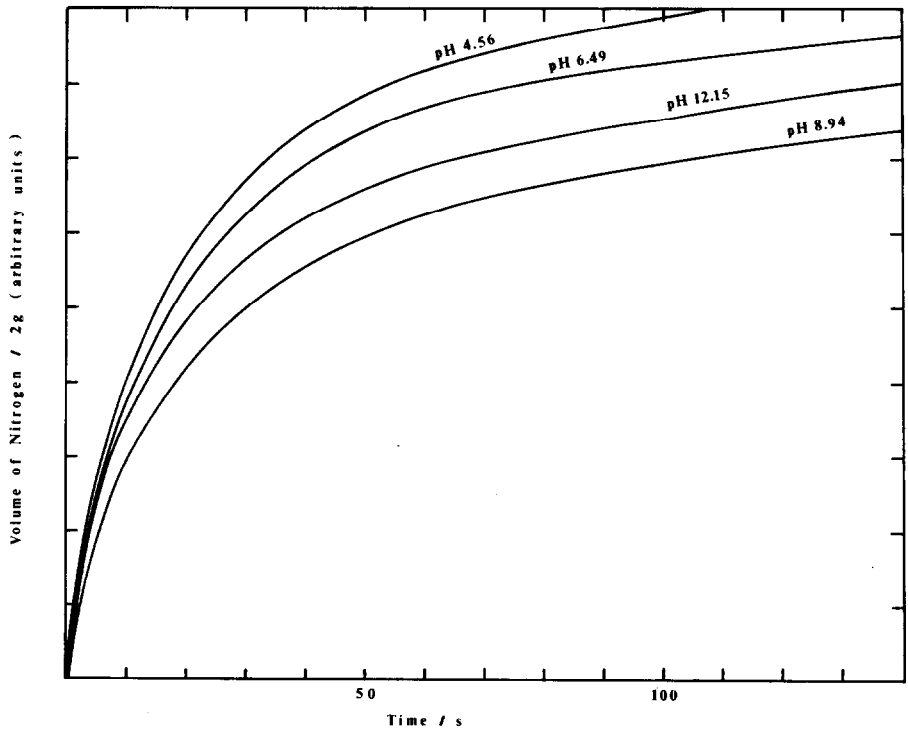

Fig. 13. Kinetic curves for the variation with time of the volume of nitrogen liberated by the reaction of hydrazine solution at 20 °C and ICS4 at different pH values; $[N_2H_4 \cdot H_2O] = 3.66_5 \times 10^{-1}$ mol dm^{-3}.

With pH values in the range 9 - 12 the reduction was found to be faster at the highest pH values, whereas at pH values between 4.5 and 9 the reduction rates were higher in the acidic media, *i.e.*, the reaction was faster at the lower pH values. This suggests an acid-catalysed reaction since, thermodynamically, the reducing power of N_2H_4 is higher than that of $N_2H_5^+$ as can be seen from the following standard redox potentials, E^0, in volts [28]:

$$N_2 + 5H^+ + 4e^- \longrightarrow N_2H_5^+ \quad -0.23 \tag{7}$$

$$N_2 + 4H_2O + 4e^- \longrightarrow N_2H_4 + 4OH^- \quad -1.15 \tag{8}$$

The effect which the ICS4 particle size has on the hydrazine reduction rate was studied at 20 °C. One gram samples which had been graded to a specific size, and an unsieved sample, were suspended in 10 ml of water, 10 ml of a hydrazine solution were added and the kinetic curve was recorded. The hydrazine reduction rates of the different fractions of ICS4, together with the unsieved sample, are depicted in Fig. 14. This shows that the reduction rate of ICS4 increased as the particle size decreased, which demonstrated the significance of the real rather than the BET surface area. A similar effect for the real external surface area has been observed for the reduction rates of sieved R2 by hydrazine [10] and for the kinetics of the leaching of reduced MnO_2 with pyrophosphate solution [29]. The high reduction rate of the unsieved sample, compared with that of the +75 μm fraction in Fig. 14, may be because it contains 22.1% and 34.4% of the two finest fractions.

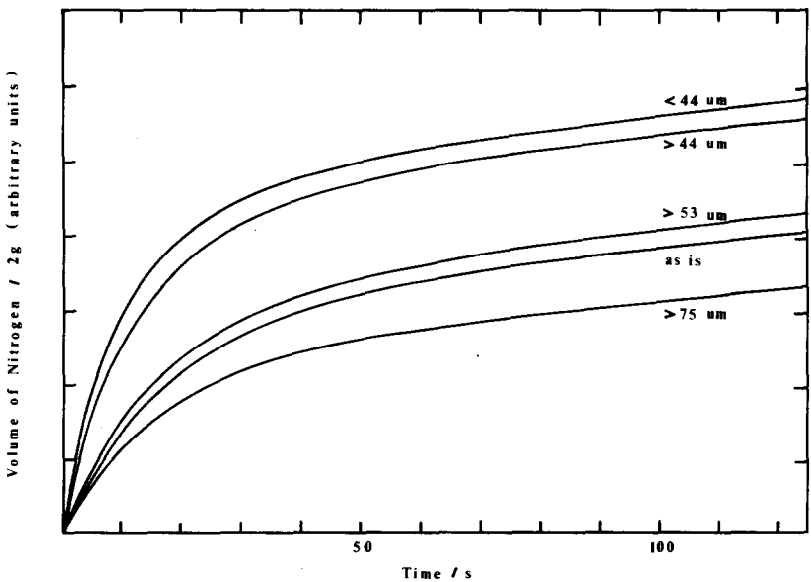

Fig. 14. Kinetic curves for the variation with time of the volume of nitrogen liberated by the reaction of hydrazine solution at 20 °C and screened ICS4; $[N_2H_4 \cdot H_2O] = 3.66_5 \times 10^{-1}$ mol dm^{-3}.

The results of tests in which the MnO_2/N_2H_4 ratio was varied so that 1 or 2 g of ICS4 was reduced by the same amount of hydrazine suggests that the kinetics of the reaction are largely determined by the available surface area. Doubling the volume of hydrazine solution to reduce 1 g of ICS4 under otherwise identical conditions only has a minor effect on the reduction rate, suggesting that the kinetics of the process are largely determined by the solid.

Acknowledgements

Thanks are due to Dr M. A. Malati for helpful discussions, and to the former Berec Group Technical Centre, U.K. for donating the commercial electrodeposited γ-MnO_2. Thanks are also due to Dr E. Preisler, Hoechst AG, W. Germany, for supplying the fibrous samples. International Common Samples were supplied by I. C. MnO_2 Sample Office, Cleveland, U.S.A.

References

1 G. G. Rao and V. N. Rao, *Z. Anal. Chem., 147* (1955) 338.
2 M. W. Rophael, L. B. Khalil and M. A. Malati, in L. J. Pearce (ed.), *Power Sources 10, (Proc. 14th Int. Power Sources Symp., Brighton, 1984)*, 1985, p. 237.
3 G. V. Rao, K. C. Rajanna and P. K. Saiprakash, *Z. Phys. Chem. (Leipzig), 263* (1982) 622.
4 W. Feitknecht, N. R. Oswald and U. Feitknecht-Steinmann, *Helv. Chim. Acta, 43* (1960) 1947.
5 J. P. Gabano, B. Morignat and J. F. Laurent, *Electrochem. Technol., 5* (1967) 531.
6 J. P. Gabano, J. Seguret and J. F. Laurent, *J. Electrochem. Soc., 117* (1970) 147.
7 G. Coeffier and J. P. Brenet, *Bull. Soc. Chim. Fr., No. 11* (1964) 2835.
8 C. Drotschmann, *Batterien, 20* (1966) 887.
9 M. W. Rophael, W. E. Mourad and L. B. Khalil, *J. Appl. Electrochem., 10* (1980) 315.
10 M. W. Rophael, *Surf. Technol., 16* (1982) 235.
11 W. C. Maskell, J. E. A. Shaw and F. L. Tye, *Electrochim. Acta, 26* (1981) 1403.
12 W. E. Mourad, M. W. Rophael and L. B. Khalil, *J. Appl. Electrochem., 10* (1980) 309.
13 G. Gattow, *Batterien, 15* (1961) 163.
14 L. B. Khalil, *Ph.D. Thesis*, Cairo University, 1986.
15 M. A. Malati and M. W. Rophael, *Lab. Pract., 27* (1978) 572.
16 M. A. Malati, *Educ. Chem., 14* (1977) 146.
17 J. Brenet, P. C. Picquet and J. Y. Welsh, in B. Schumm, Jr., H. M. Joseph and A. Kozawa (eds.), *Manganese Dioxide Symposium*, Vol. 2, I. C. MnO_2 Sample Office, Cleveland, OH, 1981, p. 214.
18 S. P. Mushran, M. C. Agrawal, R. M. Mehrotra and R. Sanehi, *J. Chem. Soc., Dalton Trans., 14* (1974) 1460.
19 K. C. Rajanna, Y. R. Rao and P. K. Saiprakash, *Indian J. Chem., Sec. A, 17* (1979) 66.
20 M. A. Malati and A. P. Peirce, to be published 1987.
21 W. C. Pickering, *Rev. Pure Appl. Chem., 16* (1966) 185.
22 L. Pons and J. Brenet, *C. R. Acad. Sci., 260* (1965) 2483.

23 T. Våland, *J. Power Sources, 1* (1976/77) 65.
24 C. L. Gardner, *J. Power Sources, 1* (1976/77) 73.
25 R. G. Burns and V. M. Burns, in A. Kozawa and R. J. Brodd (eds.), *Manganese Dioxide Symposium*, Vol. 1, I. C. MnO_2 Sample Office, Cleveland, OH, 1975, p. 306.
26 K. W. Cha, H. C. Lee and L. M. Kwon, *Hwahak Konghak, 14* (1976) 377; *Chem. Abstr. 86* 128011x (1977).
27 Y. Fukumoto, T. Matsunaga and T. Hayashi, *Electrochim. Acta, 26* (1981) 631.
28 R. B. Heslop and K. Jones, *Inorganic Chemistry*, Elsevier, Amsterdam, 1976, p. 281.
29 M. A. Malati, M. W. Rophael and I. I. Bhayat, *Electrochim. Acta, 26* (1981) 239.